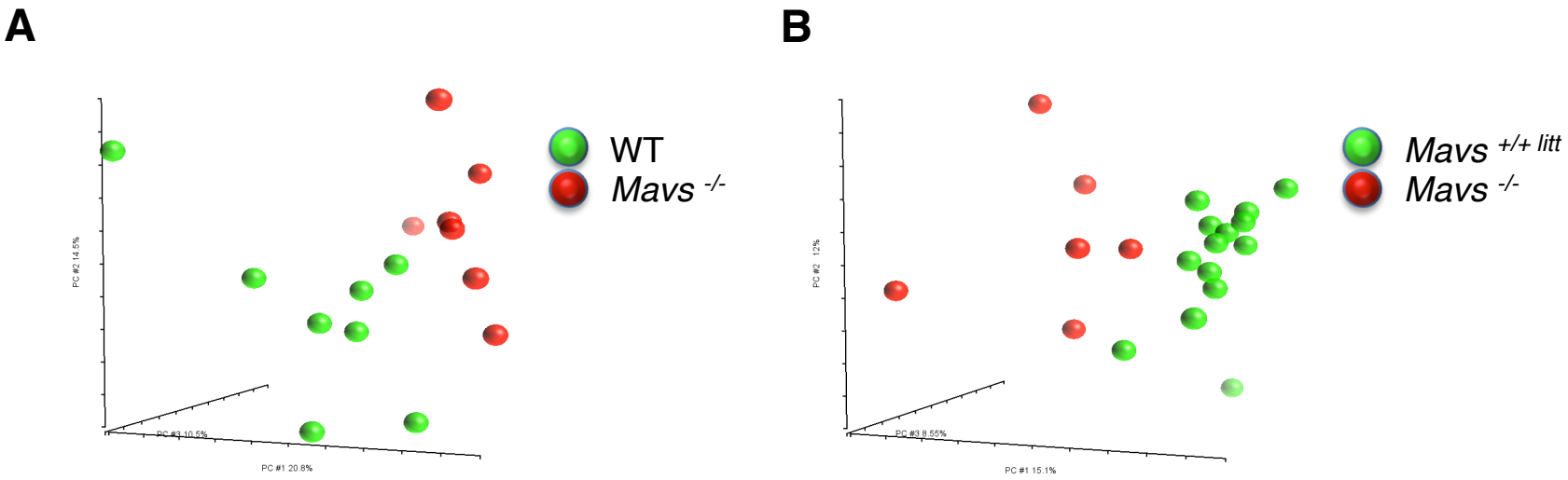

Supplementary Figure 1 *Mavs*$^{-/-}$ mice have gut microbiota dysbiosis.
(**A**,**B**) Individual experiments (from combined **Figure 1A**). (**A**) Experiment 1 was performed on *Mavs*$^{-/-}$ and B6J mice. (**B**) Experiment 2 was performed on *Mavs*$^{-/-}$ and *Mavs*$^{+/+\ litt}$ mice separated for 2 generations. Experiments 1 and 2 were done with an interval of about 1 year apart.

www.pnas.org/cgi/doi/10.1073/pnas.1722372115

Plantamura et al, Figure S2

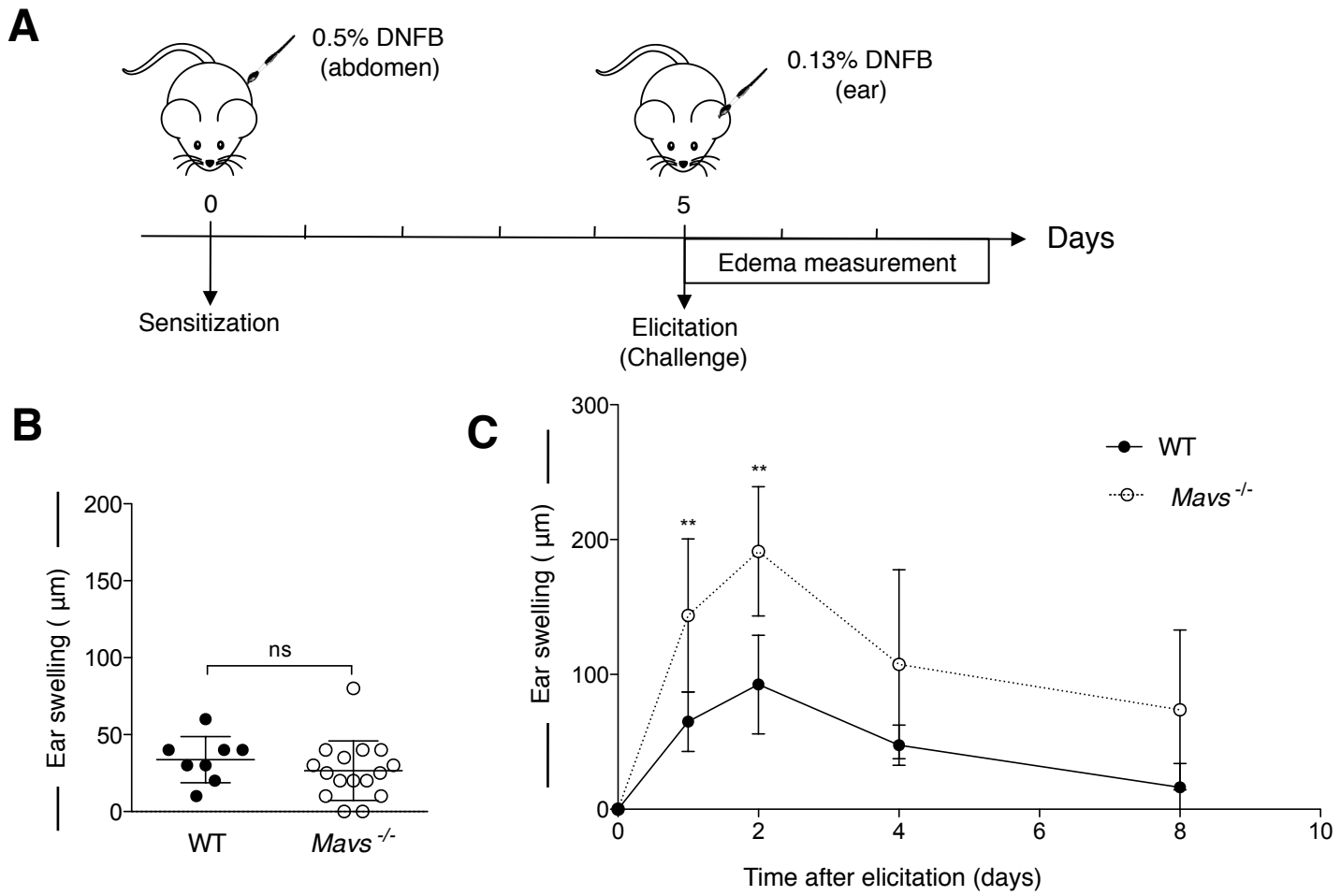

Supplementary Figure 2 Kinetics of ear swelling after DNFB challenge in WT and *Mavs*$^{-/-}$ mice. (**A**) Scheme of DTH to DNFB experimental protocol. Mice were sensitized epicutaneously on shaved abdomen with 25 µL 0.5% DNFB diluted in acetone-olive oil on day 0. On day 5, DNFB-sensitized and control unsensitized mice were challenged with 5 µL 0.13% DNFB on both sides of one ear. Control ear was painted with vehicle alone. The increase in ear swelling was measured at different time points after challenge using a spring-loaded micrometer. (**B**) To evaluate acute hapten-induced tissue irritation, background swelling was measured in non-sensitized mice 24 hours after DNFB challenge. Data presented are mean values ± SDs from one representative experiment among 15 with (n=8) WT and (n=15) *Mavs*$^{-/-}$ mice. (**C**) The ear swelling was measured every day after DNFB challenge in WT and *Mavs*$^{-/-}$ mice (n=8). Data presented are mean values ± SDs from one representative experiment among 15. Ns, non significant, ** P <0.01 as determined by Mann Whitney non parametric test.

Plantamura et al, Figure S3

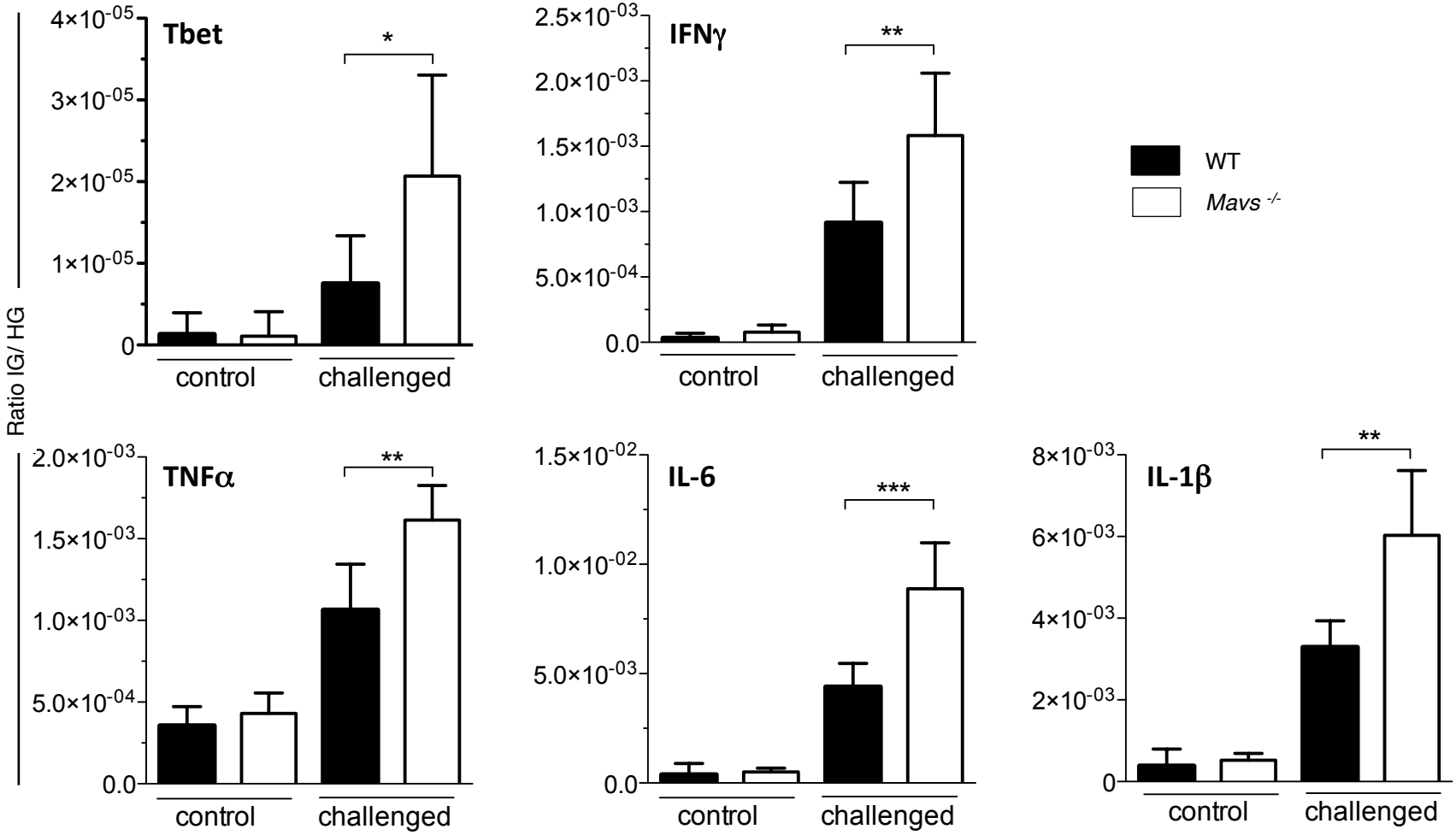

Supplementary Figure 3 Transcript levels in ear of WT and *Mavs*$^{-/-}$ mice 24h post-challenge. mRNA levels of cytokines (IFNγ, TNFα, IL-6, IL-1β) and Tbet transcription factors in challenged ear were analyzed by RT-qPCR at 24h post-challenge. Values were normalized to RPS11 mRNA levels. Results are mean values ± SDs of 1 representative experiment with n=5 WT and n=6 *Mavs*$^{-/-}$ mice). * $P < 0.05$, ** $P < 0.01$, ***$P < 0.001$, as determined by Mann-Whitney non-parametric test.

Plantamura et al, Figure S4

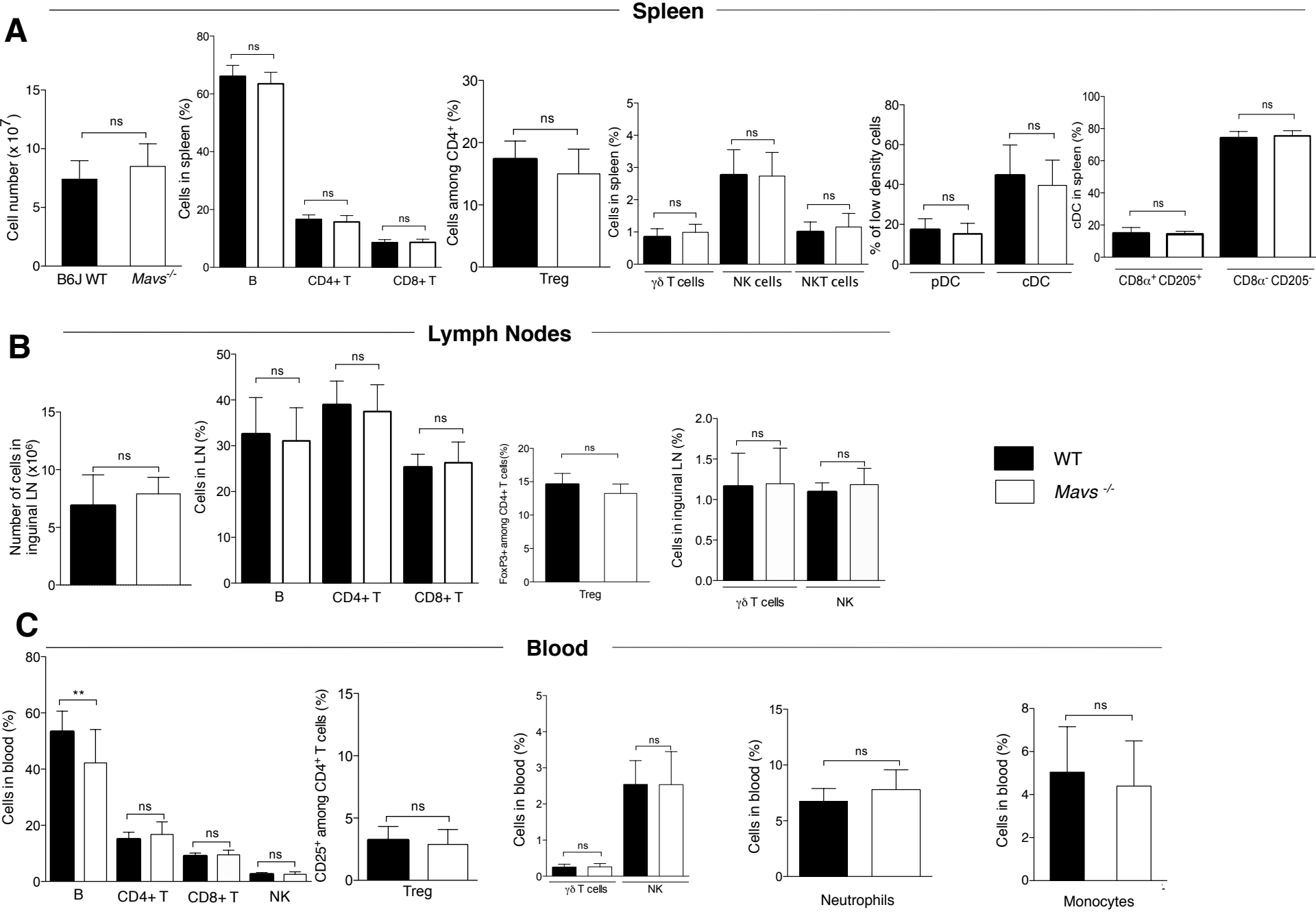

Supplementary Figure 4 MAVS deficiency does not affect leukocyte homeostasis at steady state. To study the immune system of *Mavs*$^{-/-}$ mice, we performed a deep phenotype of leukocytes subpopulations by flow cytometry in the spleen (**A**), in the inguinal lymph nodes (LN) (**B**) and in the blood (**C**). Numeration of total cells and percentage of leukocyte subpopulations were determined using surface and intracellular markers as follow: B lymphocytes (B220^{+}), CD4^{+} lymphocytes (CD3^{+} CD4^{+}), CD8^{+} lymphocytes (CD3^{+} CD8^{+}), regulatory T cells (CD3^{+} CD4^{+} FoxP3^{+}, Treg), γδ T cells (CD3^{+} TCRγ/δ $^{+}$), NK cells (NK1.1^{+} CD3^{-}), NKT cells (CD3^{+} NK1.1^{+}), pDC (CD11c^{+} B220^{+}), cDC (CD11c^{+} B220^{-}), neutrophils (CD45^{+} CD11b^{+} Ly6G^{+}), monocytes (CD45^{+} CD115^{+}). For DC analysis in spleen, low-density cells were isolated over Optiprep (Abcys). Results are mean values ± SDs of 3 (**A**), 2 (**B**) and 6 (**C**) independent experiments with n=8 mice per experiment. Ns, non significant, ** P <0.01 as determined by Mann Whitney non-parametric test.

Plantamura et al, Figure S5

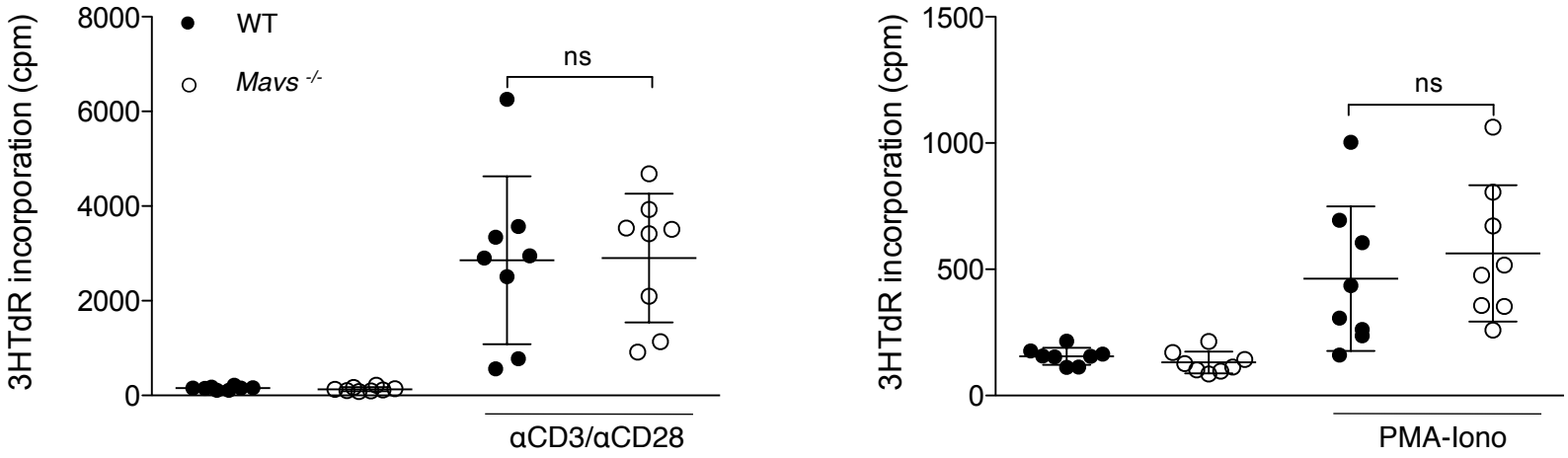

Supplementary Figure 5 MAVS deficiency does not affect T cell proliferation. T cells (5×10^4 cells/well) from WT and *Mavs*$^{-/-}$ spleens were stimulated with PMA (1 ng/ml) plus ionomycin (1 µg/ml) or with coated anti-CD3 (10 µg/ml) plus anti-CD28 (2 µg/ml) and proliferation was assessed by 3H-thymidine incorporation after 48h of culture. Results are presented with mean values ± SDs of 3 independent experiments with n=8 mice. Ns, non significant as determined by Mann Whitney non-parametric test.

Plantamura et al, Figure S6

A

	AVERAGE			SD			SEM		
	Mavs $^{+/+}$	*Mavs* $^{+/-}$	*Mavs* $^{-/-}$	*Mavs* $^{+/+}$	*Mavs* $^{+/-}$	*Mavs* $^{-/-}$	*Mavs* $^{+/+}$	*Mavs* $^{+/-}$	*Mavs* $^{-/-}$
straight	32	32	31	10.836	8.901	8.542	3.612	2.967	2.847
zigzag	45	46	47	14.392	10.448	10.006	4.797	3.482	3.3353
auchen	23	22	22	7.611	4.506	7.659	2.537	1.502	2.553

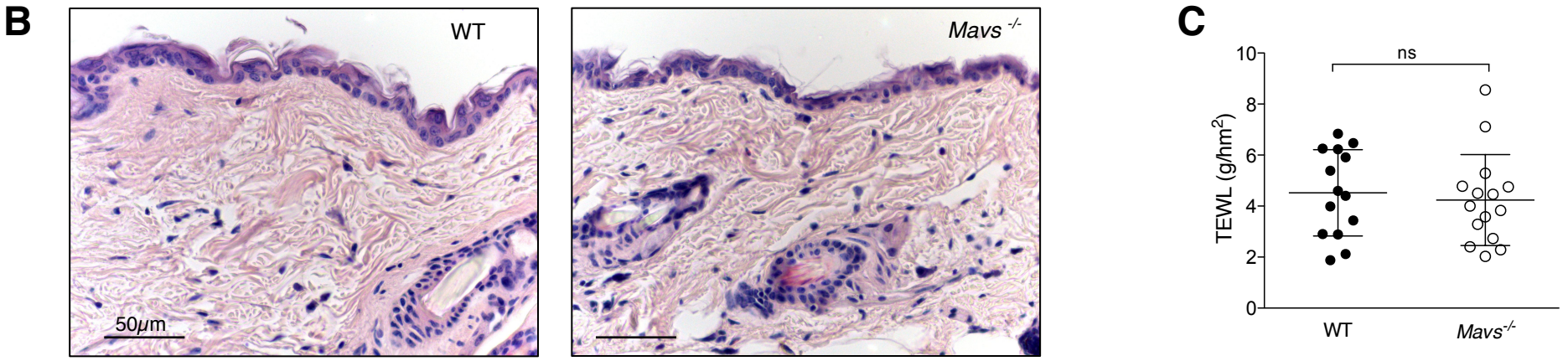

Supplementary Figure 6 *Mavs*$^{-/-}$ mice have normal skin structure and permeability. (**A**) Hairs from *Mavs* littermates were plucked from the mouse back skin and examined with a stereomicroscope. In the mouse coat, four hair types can be distinguished. Awl and guard hairs are straight and the latter are longer. Auchen and zigzag hairs have one or multiple bends, respectively. Based on these morphological hallmarks the presence of the different hair types was determined among 60 and 130 hairs. (**B**) Skin samples from WT and *Mavs*$^{-/-}$ mice (n=6) were fixed, stained with Haematoxylin & Eosin and observed by microscopy. Histologic analysis revealed no apparent abnormalities at structure level. Epidermal thickness and differentiation appeared normal and ectodermal appendages, like hair follicles and sebaceous glands, displayed a normal architecture. (**C**) Transepidermal Water Loss (TEWL) was measured on shaved skin from WT (n=6) and *Mavs*$^{-/-}$ mice (n=5) at steady state (2 to 4 measurements per mice) to evaluate skin permeability. Ns, non significant as determined by Mann Whitney non-parametric test.

Plantamura et al, Figure S7

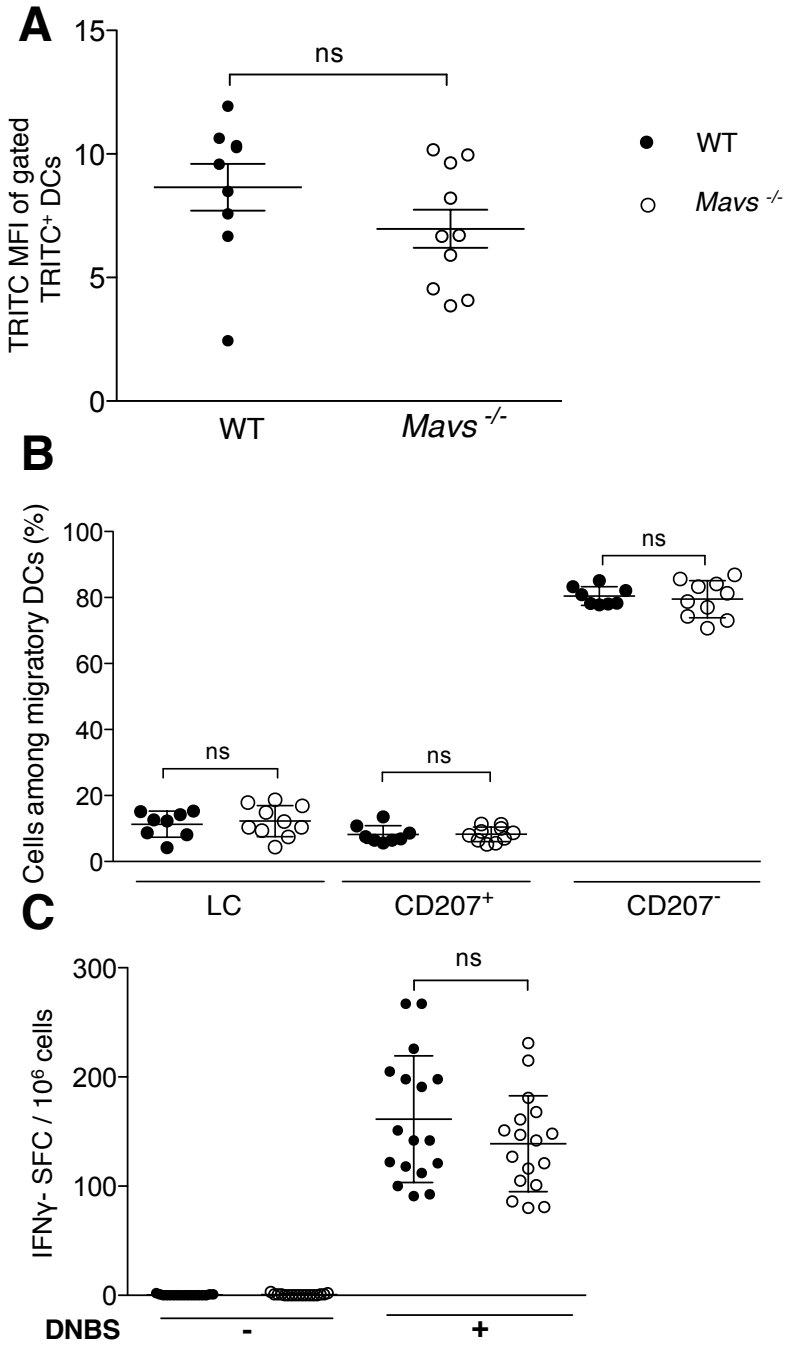

Supplementary Figure 7 Mavs deficiency does not affect hapten-uptake, DC migration and T cell priming. (**A**,**B**) To evaluate hapten-uptake and DC migration from skin to dLNs, we performed classical migration experiment by applying the fluorescent dye TRITC (tetramethylrhodamine-5-(and-6)-isothiocyanate) with skin irritant DBP (dibutilphtalate) on ear of WT and *Mavs*$^{-/-}$ mice and harvested auricular dLNs after 48 hours (96 hours, data not shown). TRITC uptake was evaluated by TRITC Median of Fluorescence Intensity (**A**). CD11c^{+} TRITC^{+} cells were analyzed by flow cytometry and the percentage of Langerhans cells (LC, CD207^{+} CD 103^{-}) and dermal DCs (CD207^{+} CD103^{+} and CD207^{-} CD103^{-}) were determined (**B**) Results are presented with mean values ± SDs of 2 independent experiments with n=4 WT and n=5 *Mavs*$^{-/-}$ mice. (**C**) ELISPOT assay was performed to estimate the number of antigen specific IFNγ producing cells. Axillary and Inguinal dLNs were collected 5 days post-sensitization with DNFB. Isolated cells were plated and incubated at 37°C for 20h, with or without soluble analog of DNFB, DNBS (Dinitrobenzene sulfonic acid, 4mM). Numbers of IFNγ spots are presented with mean ± SEMs, representative of 1 experiment among 4 with n=5 mice. Ns, non significant as determined by Mann Whitney non-parametric test (**A**,**B**,**C**).

Plantamura et al, Figure S8

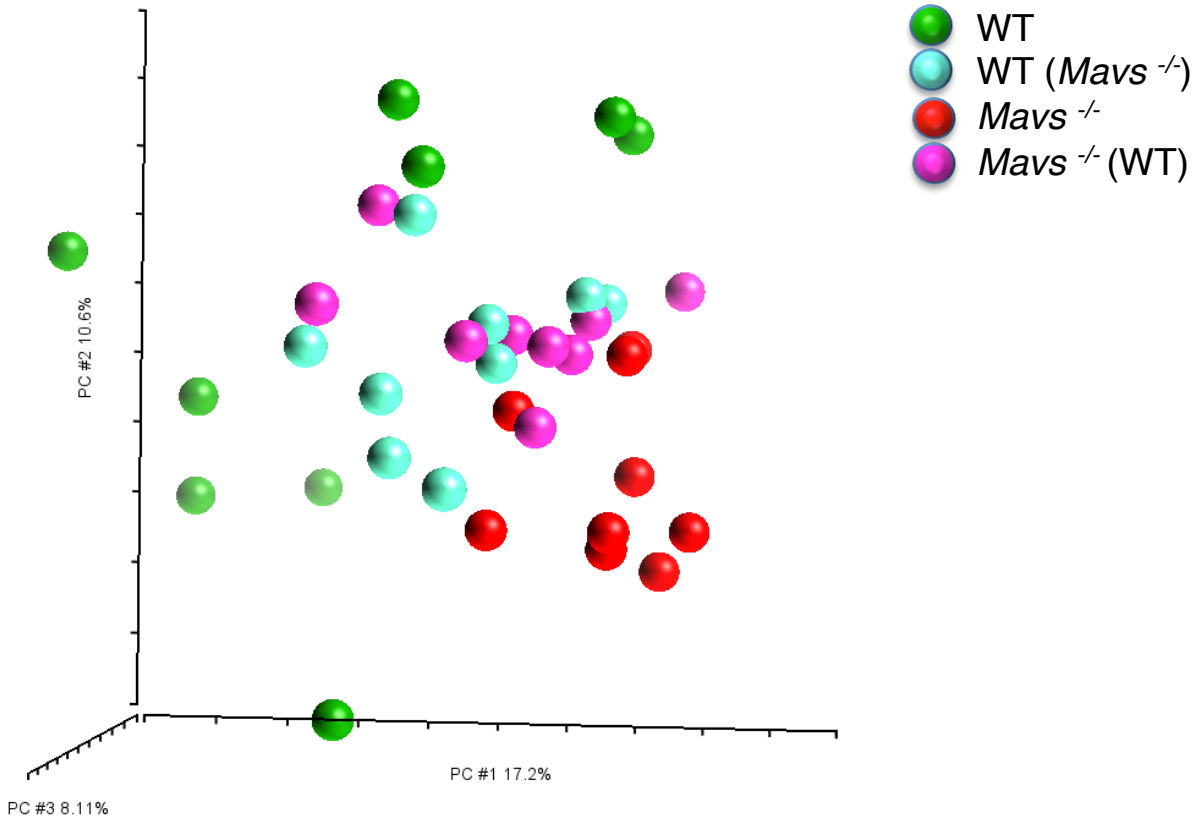

Supplementary Figure 8 Co-housed WT and *Mavs*$^{-/-}$ mice acquire microbial composition, which is similar to both WT and *Mavs*$^{-/-}$ animals, confirming that co-housing in our system results in sharing of microbial species between animals. Animals were co-housed in 50/50 ratio for 4 weeks prior to analysis. Faecal samples were analysed using MiSeq sequencing machine. PCA plot demonstrates similarities/differences between microbial communities of WT (green circles), Co-housed WT (cyan circles), *Mavs*$^{-/-}$ (red circles) and *Mavs*$^{-/-}$ co-housed (magenta circles) animals.

Plantamura et al, Figure S9

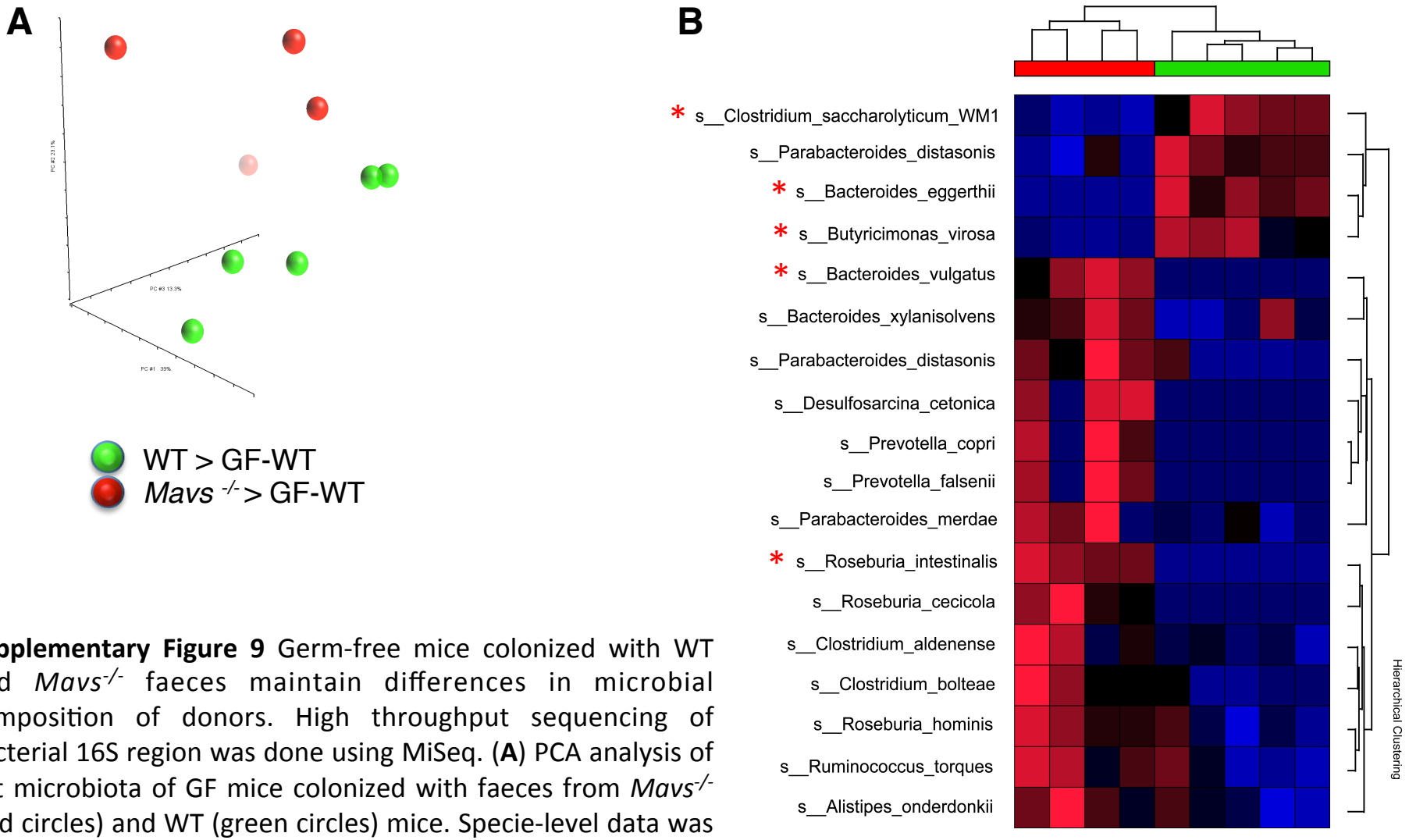

Supplementary Figure 9 Germ-free mice colonized with WT and *Mavs*$^{-/-}$ faeces maintain differences in microbial composition of donors. High throughput sequencing of bacterial 16S region was done using MiSeq. (**A**) PCA analysis of gut microbiota of GF mice colonized with faeces from *Mavs*$^{-/-}$ (red circles) and WT (green circles) mice. Specie-level data was used to construct PCA plots. (**B**) Heatmap visualization of the results of specie-level comparison between gut microbiota of WT > GF-WT and *Mavs*$^{-/-}$ > GF-WT mice. Significance was determined by Student's *t*-test. Species with p-value<0.05 are shown, red asterisk indicate species with q-value <0.1.

Plantamura et al, Figure S10

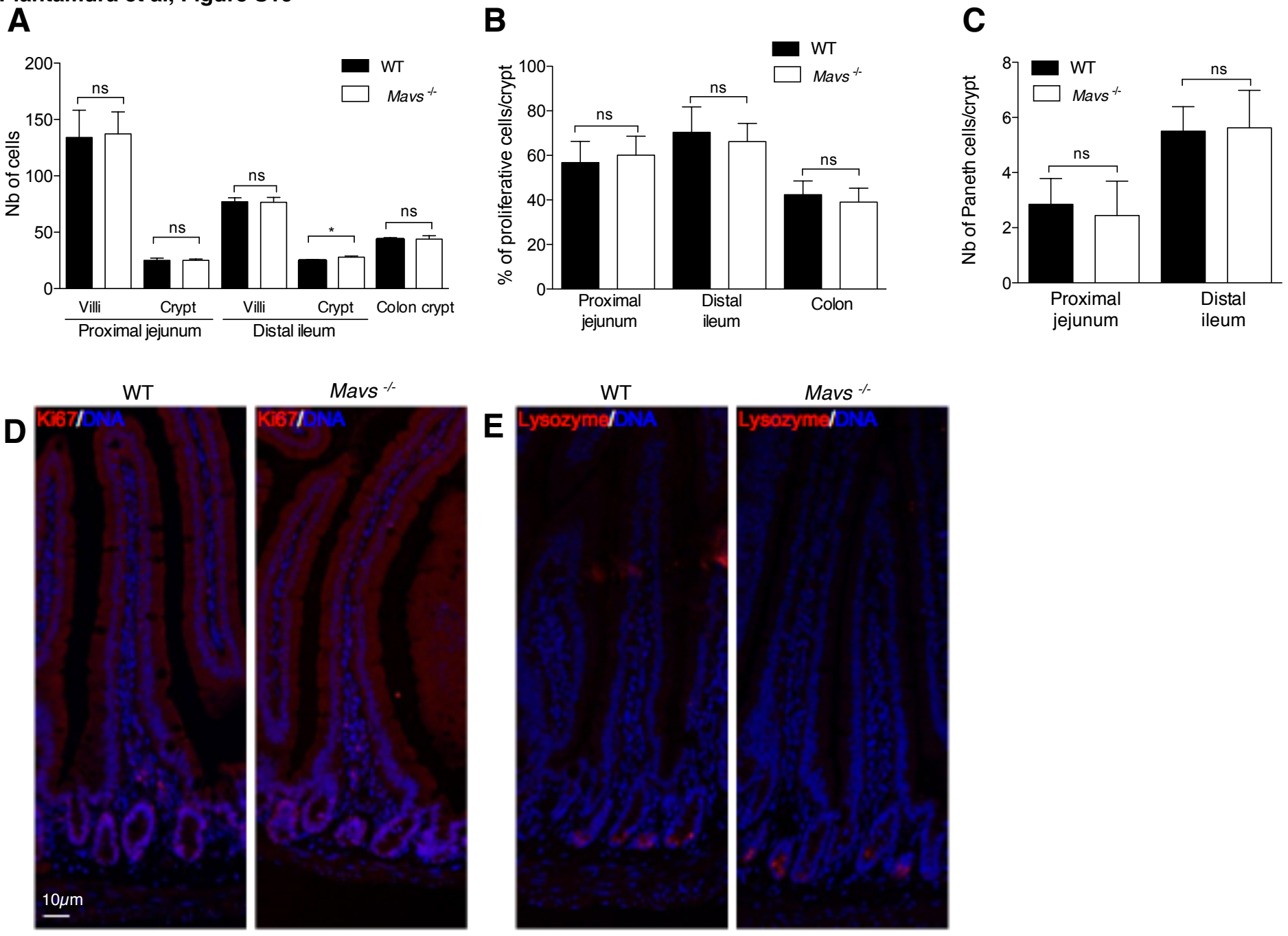

Supplementary Figure 10 *Mavs*$^{-/-}$ mice have normal gut epithelial properties (**A**) Quantification of the number of epithelial cells along the crypt-villus axis in the proximal jejunum, distal ileum and colon mucosa of WT (n=5) and *Mavs*$^{-/-}$ mice (n=5). Bars represent the mean values ± SD. A minimum of 5 well-oriented axes from 3 different animals per genotype were counted under the microscope from histological sections. (**B**) Quantification of the percentage of Ki67 positive proliferative cells in the crypts of proximal jejunum, distal ileum and colon of WT and *Mavs*$^{-/-}$ mice. Bars represent the mean percentages ± SD. A minimum of 10 well-oriented crypts from 2 different animals per genotype were counted under the microscope. (**C**) Quantification of the number of lysozyme positive Paneth cells in the crypts of proximal jejunum and distal ileum of WT and *Mavs*$^{-/-}$ mice. Paneth cells are absent from the colon. Bars represent the mean percentages ± SD. A minimum of 10 well-oriented crypts from 2 different animals per genotype were counted. (**D-E**) Example of confocal images of WT and *Mavs*$^{-/-}$ proximal jejunum immunolabelling for DNA, Ki67 (**D**) and Lysozyme (**E**). Ns, non significant as determined by Mann Whitney non parametric test.